SPANDIDOS PUBLICATIONS EXPERIMENTAL AND THERAPEUTIC MEDICINE 11: 2489-2494, 2016

Effect of electroacupuncture on gastric interstitial cells of Cajal in a rat model of diabetic gastroparesis

GUOHUA LIN[1], JIAWEI ZHANG[2], LIXIA LI[3], ZHUOCHENG ZOU[4], CHUYUN CHEN[3], LIFEI XUE[4] and LANFENG ZHAO[1]

[1]Department of Acupuncture, The First Affiliated Hospital of Guangzhou University of Chinese Medicine; [2]College of Acupuncture and Moxibustion, Guangzhou University of Chinese Medicine, Guangzhou, Guangdong 510405; [3]Department of Acupuncture, Guangzhou Hospital of Traditional Chinese Medicine, Guangzhou, Guangdong 510130; [4]Department of Acupuncture and Moxibustion, The First Affiliated Hospital of Guangxi University of Chinese Medicine, Nanning, Guangxi 530023, P.R. China

Received September 3, 2014; Accepted July 17, 2015

DOI: 10.3892/etm.2016.3185

Abstract. The aim of the present study was to observe the effect of electroacupuncture (EA) on the gastric interstitial cells of Cajal (ICCs) in a rat model of diabetic gastroparesis (DGP). The gastric tissues were collected from 75 rats, which had been divided into three equal groups (n=25/group): Blank, model and EA. Hematoxylin and eosin and immunohistochemical staining were used to observe the cellular morphology and distribution of c-kit-positive gastric ICCs; light microscopy was used to count the number of ICCs; and electron microscopy was used to observe the ultrastructure of the rat ICCs. Compared with the model group, the gastromucosal glandular and smooth muscle cells of the EA group were more regularly arranged, with fewer vacuoles; there was an increased cellular gap and the vacuolar degeneration on the gastric walls was mild. Image analysis showed that the blank group exhibited the greatest number of c-kit-positive ICCs, and the number of c-kit-positive ICCs in the blank group was significantly different from that in the model and EA groups ($P<0.01$): Blank group > EA group > model group. In conclusion, DGP rats exhibited a reduced number of gastric ICCs, altered ultrastructural morphology and a reduced number of cell organelles, particularly mitochondria, compared with the blank group. EA may help to reverse the various pathological changes of gastric ICCs in rat models of DGP.

Correspondence to: Dr Lixia Li, Department of Acupuncture, Guangzhou Hospital of Traditional Chinese Medicine, 16 Zhuji Road, Guangzhou, Guangdong 510130, P.R. China
E-mail: lixialicn@163.com

Key words: experimental study, interstitial cells of Cajal, diabetic gastroparesis, electroacupuncture

Introduction

Gastroparesis is a common symptom in patients with a long history of diabetes. Between 30 and 50% of patients that have had diabetes for >10 years exhibit such symptoms of gastric neuromuscular dysfunction as satiety, weight loss, abdominal pain, distension and discomfort, nausea and vomiting. Neuropathological changes, a reduction in the number of gastrointestinal interstitial cells of Cajal (ICCs), morphological changes, hyperglycemia, microvascular diseases, microcirculatory disorders, gastrointestinal hormone changes and *Helicobacter pylori* are all believed to be involved in the pathogenesis of diabetic gastroparesis (DGP) (1-7). The inherent gastric nerves have recently been subject to significant focus, and it has been suggested that the most important mechanism of DGP is the deficiency of neuronal nitric oxide synthase expression and the reduction of ICCs (1-7).

Electroacupuncture (EA) is a method which stimulates the acupoints via electric currents using acupuncture needles. Compared with manual acupuncture, EA is more readily controllable and easier to standardize, and it allows stronger and more continuous stimulation with less pain and tissue damage (8). In addition, its effects are more rapid and longer lasting (8). Studies have indicated that, EA can effectively reduce the symptoms of gastroparesis, including nausea, vomiting and abdominal distension, and promote gastric emptying in patients with diabetes (9,10). Furthermore, EA has been shown to increase the number of ICCs in the colons of slow-transit constipated rats (11); EA stimulation towards 'Zusanli', one of the most frequently used acupuncture points, may increase the electrical activity of ICCs, thus improving the gastric electrical activity and increasing the gastric motility (12,13). It has yet to be fully elucidated, however, whether the alleviation of DGP symptoms in rats by EA is associated with improvements in the gastric neuromuscular function and alterations in the numbers and morphology of gastric ICCs. The present study investigated the effect of EA on the numbers and morphology of gastric ICCs, with the aim of exploring the mechanism of EA and facilitating its potential use in alleviating the symptoms of patients with DGP.

Materials and methods

Animal models. Male Sprague Dawley rats, aged 8 weeks and each weighing 180-220 g, were provided by the Experimental Animal Center of Guangzhou University of Chinese Medicine, (Guangzhou, China; certificate no. 0055684). The rats were bred in a specific-pathogen-free laboratory and left to adapt for 3 days under a 12-h light/dark cycle, with the temperature at 20-28˚C and the humidity at 75-90%. The rats were fed a normal diet, with free access to drinking water. Following adaptation, 25 of the rats were randomly allocated to the blank group and fed the basal diet, while the remaining rats (n=50) were fasted for 12 h. Streptozotocin (STZ; Sigma-Aldrich, St. Louis, MO, USA) was dissolved in 0.l mmol/l sodium citrate buffer (pH 4.5; Guangzhou Chemical Reagent Factory, Guangzhou, China; batch no. 20081202-2) to prepare a 1% solution. The solution was then intraperitoneally injected in one step into the 50 rats (50 mg/kg). Two days later, the fasting blood glucose (FBG) of the rats was measured using an Accu-Chek® Advantage blood glucose meter and test strip (Roche, Indianapolis, IN, USA). If the 72-h FBG was >200 mg/dl and persisted at this level for 2 weeks, it indicated that the diabetes model was successfully established (14,15). A high-fat, high-sugar diet was then fed to the model rats in accordance with the irregular diet method, in which the rats were fed the high-fat diet on the morning of an odd date and the afternoon of an even date, for 10 weeks.

There were significant differences in gastrointestinal propulsive indicators between the model and blank groups; the gastrointestinal propulsive indicators were calculated using the following formula: Gastrointestinal propulsive rate = [distance from C-powder front to pyloric sphincter (cm)/distance from pyloric sphincter to end of small intestine (cm)] x100% (statistical method: One-way analysis of variance). These differences, taken together with the changes in the stool quantity and characteristics, indicated that the DGP model was successfully established. Following the successful establishment of the DGP model, the rats were then randomly divided into the model group (without any treatment) and the EA group (EA treatment once/day for 5 continuous days, followed by 2 days rest, for a total of 19 days). Each group contained 25 rats.

Treatment method. Each EA rat was placed in the homemade rat fixer, and the acupoints of Housanli, Zhongwan and Weiyu were disinfected with 75% alcohol. The disinfection was performed on the left and right sides in turn, and the acupoint selection method was based on the 'Experimental Animal Acupoint Map' developed by Hua *et al* (16). Sterile acupuncture needles were selected (Qiu model 30; needling depth, 0.76-1.0 cm; Suzhou Huatuo Medical Supplies Company, Suzhou, China). EA was performed with a Han's Acupoint Nerve Stimulator (LH202H; Shanghai TCM Co., Ltd., Shanghai, China); the stimulating waveforms used 15-Hz waves, and the intensity was set to make the acupoint skin jitter slightly. The needle was maintained for 15 min. Following the treatment, the rats could eat normally.

Sample collection and handling. Following the EA treatment, the rats underwent spinal dislocation, followed by a laparotomy to obtain a rectangular strip of antrum (2.0x0.5 cm^2). The antrum was placed in 10% neutral formalin for the fixation, and then dehydrated, paraffin-embedded and sliced into sections (a total of four consecutive slices, each with a thickness of 4 μm). The slices were dried at 60˚C for 30 min, and two samples from each rat were randomly selected for hematoxylin and eosin (HE) staining. The 4-μm sections were dewaxed using xylene, dehydrated with graded alcohol, stained with 1% HE and then rinsed with twice-distilled water, dehydrated, hyalinized, dried and mounted using neutral gum.

Immunohistochemical staining. In order to assess the number and distribution of the ICCs, the samples were subjected to anti-c-kit monoclonal antibody immunohistochemical staining (15) and observed using light microscopy. The immunohistochemical staining steps were performed at room temperature. The 4-μm thick paraffin samples were attached onto pre-coated poly-lysine slides, baked at 60˚C for l h and at then at 37˚C for 2 days. The slices were subsequently dewaxed, dehydrated and rinsed twice (for 3 min each time) with 0.0l mol/l pH 7.4 phosphate-buffered saline (PBS). The same rinsing method was performed following the steps to block the endogenous peroxidase, expose and retrieve the antigens and overnight storage at 4˚C. Endogenous peroxidase activity was blocked via incubation with hydrogen peroxide (3%) for 15 min. For antigen exposure, proteinase K was applied at 37˚C for 20 min, and the slices were then placed into the antigen retrieval box, which was filled with pH 6.0 citric acid buffer. Antigen retrieval was performed by microwaving the samples at 5,883.99 watts for 9 min. The samples were then removed and allowed to cool down to room temperature. Normal goat serum (10%) was used to block the slices for 15 min, prior to the serum being removed and the liquid surrounding the slices being dried under suction. The slices were not washed. Rabbit anti-c-Kit polyclonal primary antibody (cat. no. bs-10005R; Beijing Bioss Biosynthesis Biotechnology Co. Ltd., Beijing, China) was diluted to 1:200 with 0.01 M PBS, and pipetted onto the slice. The simple addition of 0.01 M PBS was used as the negative control. Each slice was then placed into the wet box and stored overnight at 4˚C. Goat anti-rabbit IgG secondary antibody (cat. no. bs-0295G-SA; dilution, 1:200; Beijing Donglin Changsheng Biotechnology Co. Ltd., Beijing, China) was then pipetted onto the slice, placed into the wet box and stored overnight at 4˚C. 3,3'-Diaminobenzidine was then added to the slice and observed under the light microscope for 3-10 min until positive staining could be observed. The slices were then washed with distilled water, stained, dehydrated and mounted.

Microscopy. The number and distribution of the ICCs was assessed under using light microscopy. A micrometer-scale eyepiece was installed on a light microscope (LSM 510 META laser scanning confocal microscope; Carl Zeiss AG, Oberkochen, Germany) and used for the observation of the myenteric nerve plexus and smooth muscles at low (x10) and high (x40) magnification, as well as the number and intensity of c-kit-positive cells. The 8502 image analyzer (Tracor Northern, Middleton, WI, USA) was used: Brownish yellow-stained regions were set as the positive, and the percentage of positive regions in each field was calculated to express the ICC content.

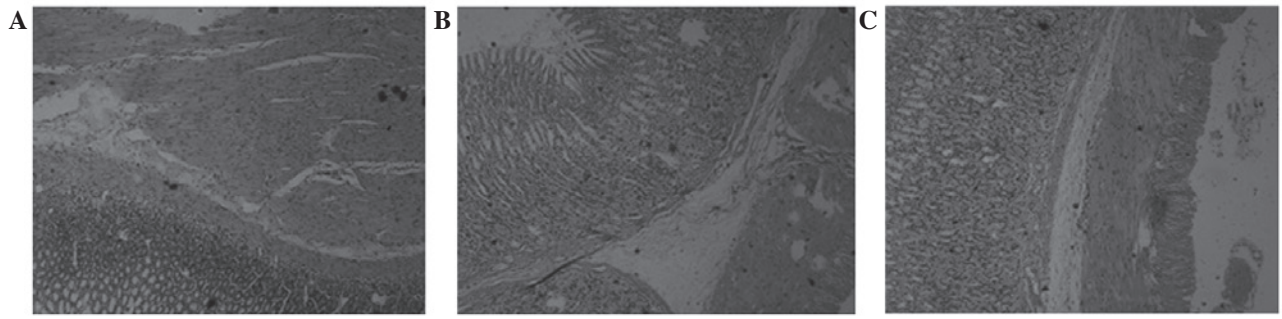

Figure 1. Hematoxylin and eosin staining of the (A) blank, (B) model and (C) electroacupuncture groups (magnification, x40).

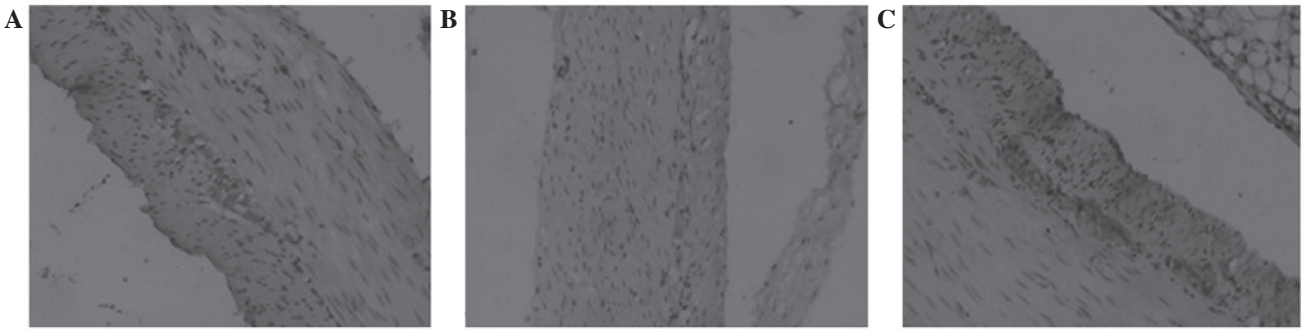

Figure 2. c-kit immunohistochemical staining of the (A) blank, (B) model and (C) electroacupuncture groups (magnification, x40).

An electron microscope (H-7500 transmission electron microscope; Hitachi, Tokyo, Japan) was used for the tissue observations. Full-layer gastric tissues (~1 cm^2; 0.5 cm to the pylorus) were cut into 1x1 mm^2 tissue blocks, and stored in ice-cold 3% glutaraldehyde for 2-4 h. The tissue samples were then rinsed with 0.1 mol/l PBS for 10 min twice, fixed with 1% osmic acid for 1.5-2 h and rinsed with 0.1 mol/l PBS for 5 min twice. Ethanol at 50 and 70% was used for the gradient dehydration, with 10 min at each level. The samples were then dehydrated with 80, 90 and 100% acetone, for 10 min at each level, twice. Epoxy resin and Epon 812 embedding agent were mixed in a ratio of 1:1 and replaced 100% acetone for 40 min; the Epon 812 was then used to soak the tissues at 37˚C overnight. The tissue blocks were subsequently embedded in the Epon 812 embedding agent and polymerized for 48 h at 60˚C. AO ultramicrotome was used to prepare 1-μm ultra thin slices (American Optical, Southbridge, MA, USA), flattened on water. The flattening procedure was performed as follows: The slices were transferred onto a drop of water added to a glass slide, heated to make the slices flat. Finally, the slices were subjected to HE staining. The slices were positioned under the dissecting and ordinary microscopes. The AO ultramicrotome was used to prepare the 40- to 60-nm ultra thin slices, and the slices were collected with a copper mesh, followed by double-staining with 70% ethanol-prepared saturated uranyl acetate and lead solution. Once the slices had dried, the slices were observed and the images recorded by electron microscopy.

Statistical analysis. All statistical analysis was carried out using SPSS 17.0 software (SPSS, Inc., Chicago, IL, USA). Data are presented as the mean ± standard deviation. The comparisons among different groups were performed using the t-test. $P<0.05$ was considered to indicate a statistically significant difference.

Results

HE staining of gastric tissues. The HE staining results are shown in Fig. 1. The gastric glandular cells and smooth muscle cells (SMCs) of the blank group were arranged regularly and tightly, with moderate intercellular gaps and no vacuolar degeneration or vascular dilation (Fig. 1A). In comparison, the glands of the model group were misaligned, the intracellular gaps were larger and the glandular cytoplasm was reduced in amount and lightly stained (Fig. 1B). Vacuolar degeneration appeared, the mucosa and submucosa were congested, the blood vessels were dilated, the cytoplasm of the muscular gastric wall was lightly stained and translucent, and vacuolar changes were exhibited compared with the control group. In the EA group, compared with the model group, the vascular congestion in the gastric mucosa and submucosa was mitigated, the mucosal gland cells and SMCs were arranged more neatly, and with fewer vacuoles, the intercellular gaps were marginally larger and only minor vacuolar degeneration was observed in the gastric wall (Fig. 1).

c-kit immunohistochemical staining

Distribution and morphology. Following the c-kit immunohistochemical staining, observation under the light microscope revealed that the cell membrane and cytoplasm of the ICCs were stained brown (Fig. 2). The positively stained ICCs were most dense in the gastric antrum of the blank group. The cells were located between the circular and longitudinal muscle layers, and between and on the inner surface of the circular

Table I. Comparison of the quantity and intensity of gastric c-kit-positive cells among the three groups.

Group	Number of positive cells	Positive area percentage
Blank	32.33±5.51	0.358±0.153
Model	18.67±6.11[a]	0.127±0.074[c]
EA	31.33±4.73[b]	0.290±0.123[d]

Data are presented as the mean ± standard deviation. [a]P<0.01 compared with blank group; [b]P<0.01 compared with model group; [c]P<0.05 compared with blank group; [d]P<0.05 compared with model group.

muscle layers, in particular between the ring and longitudinal muscle layers. The cells were mostly accompanied by nerve fiber endings and nerve bundles, and connected together tightly by gap junctions, exhibiting an aggregated distribution. The cells were generally fusiform, elongated or irregular, and exhibited numerous cell processes, little cytoplasm and large nuclei, which were mostly oval and deeply stained. The ICCs of the model group were atrophic and significantly reduced in number; the cell processes had disappeared and the cell contrasts were poor. The tight junctions between the ICCs, nerve cells and SMCs were significantly reduced. The ICCs of the EA group were marginally decreased in number compared with those of the blank group, although the cell morphology was basically normal. The cells exhibited shortened processes, and the tight junctions between the ICCs and the other cells remained.

Comparison of quantity and intensity of c-kit-positive cells in each group. Image analysis showed that the largest number of positive ICCs was found in the blank group. Statistically significant differences existed among the model, EA and blank groups: Blank group > EA group > model group (P<0.01). These findings indicated that EA regulated the number of c-kit-positive ICCs. The positive area percentage of the normal blank group was the highest (Table I).

Ultrastructural features of gastric ICCs. The gastric ICCs of the blank-group rats were mainly distributed in the myenteric nerve plexus of the circular and longitudinal muscle layers, as well as among the circular muscle cells, and they were closely linked by gap junctions. Many foveolae were distributed along the cell membrane, and the basal cell membrane was complete. In the majority of cells, large, irregular nuclei could be observed; heterochromatin was common and was distributed along and under the nuclear membrane. The structure was well-defined, with little cytoplasm. One or more processes were present, and the processes were rich in cytoplasm and organelles, particularly mitochondria, which were closely arranged inside the cytoplasm. Fully developed rough endoplasmic reticulum, smooth endoplasmic reticulum and Golgi apparatus could be observed, accompanied by numerous intermediate filaments but no rough filaments (Fig. 3).

In the model group, the gap junctions among the ICCs, SMCs and nerve endings were significantly reduced, and the structure of the surviving cells was destroyed. The cells exhibited an unclear and loosely connected structure, with an incomplete basal cell membrane that lacked continuity. Regions of the basal membrane were observed to have separated from the cell membrane and formed cavities. The numbers of intracellular organelles, e.g. ribosomes and mitochondria, were significantly reduced compared with the normal ICCs; furthermore, the mitochondria showed significant swelling, vacuolar degeneration and myelin-like degeneration or even dissolution. The endoplasmic reticulum was expended, the rough endoplasmic reticulum was degranulated and the intracellular cytoplasm had extensively dissolved, leading to considerable vacuolization inside the cytoplasm, which was mostly distributed along the vacuolar membrane. In addition, the perinuclear gaps had widened (Fig. 3).

The number of ICCs in the EA group was more than that in the model group, while slightly less than that in the control group. The morphological structure of the ICCs was basically normal, although the mitochondria were reduced in number compared with the blank group and exhibited mild swelling, and the gaps among the cells remained. The pathological damage to the ICCs, nerve endings and SMCs was less than that in the model group, and the structures were more distinct and ordered. The pathological damage to the nerves within the wall and the cell processes was also reduced compared with that in the model group, and the ICC distribution was improved. The gastric capillary walls were not smooth, while the endothelial cell swelling, as well as the luminal congestion and bending, were reduced, and the vacuolar degeneration was less (Fig. 4).

Discussion

In a diabetic state in rats, the gastric gland cells, SMCs in the gastromuscular layers, circular muscle nerve cells and ICCs exhibit varying degrees of damage. The observations in the present study revealed that, compared with normal rats, the glands were arranged in a disorderly manner, the cellular gaps were larger, the glandular cytoplasm was reduced and lightly stained, and vacuolar degeneration was apparent. The mucosa and submucosa were congested and the vascular lumens were expended. The SMCs exhibited a disordered arrangement, and several dissolved vacuoles were observed within the muscular cytoplasm. The mitochondria were swollen and exhibited vacuolar degeneration or had dissolved. The neuronal nuclei inside the myenteric plexus were dissolved and necrotic. The cytoplasm was partially dissolved, there were fewer organelles and a number of autophagic vacuoles could be observed within the cytoplasm. The reduction in the number of organelles within the ICCs was consistent with the literature (3,4,7,17).In addition, the peripheral axons and dendrites were partially swollen or dissolved, the electron density was not uniform, and vacuoles had formed. The synaptic vesicle content inside the nerve varicosity was significantly reduced, and the number of gastric ICCs was significantly decreased compared with the blank group. Furthermore, the connections among the ICCs, SMCs and nerve endings were significantly reduced, the connections among the surviving ICCs were loose, the gaps were widened and the perinuclear cytoplasm of the ICCs was

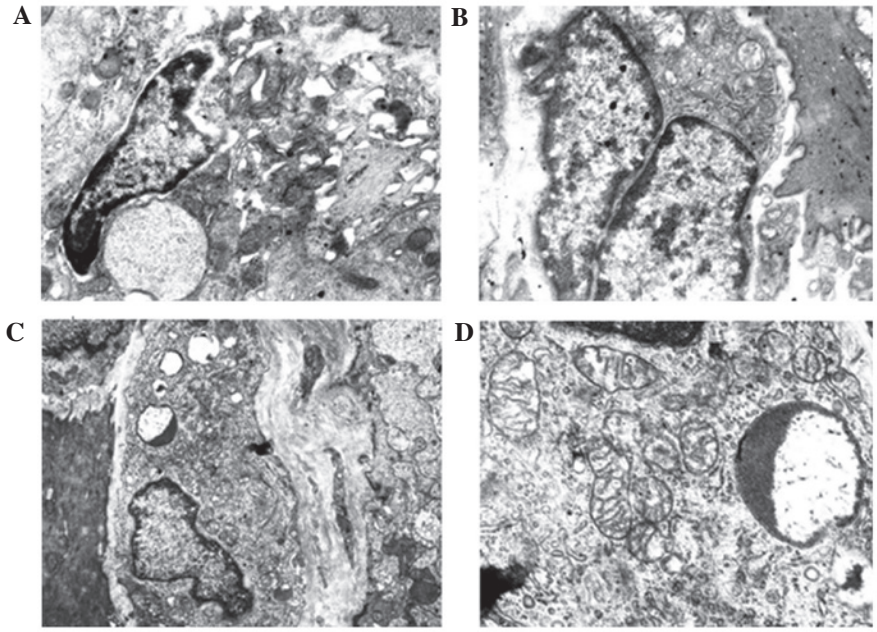

Figure 3. Ultrastructural features of the gastric interstitial cells of Cajal. (A and B) Blank group at magnifications of (A) x12,000 and (B) x10,000; (C and D) model group at magnifications of (C) x6,000 and (D) x20,000.

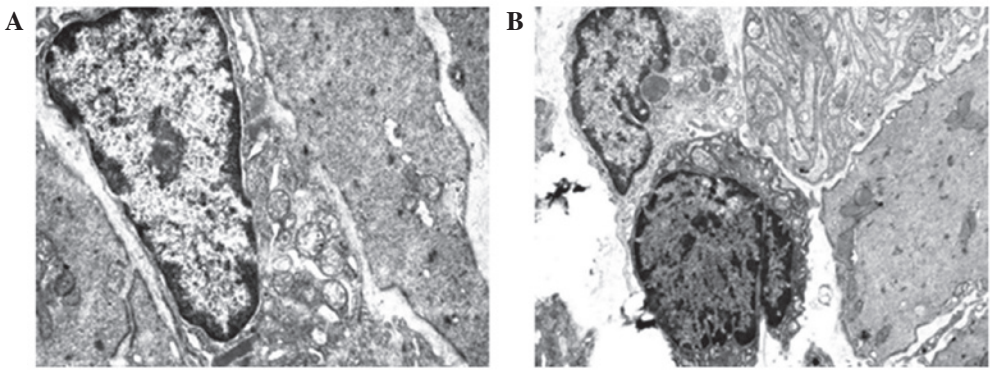

Figure 4. Ultrastructural features of the gastric interstitial cells of Cajal in the electoracupuncture group: (A) Magnification, x10,000 and (B) magnification, x6,000.

significantly reduced. The changes in the number of ICCs may have been associated with the chronic high blood sugar or insulin resistance in diabetes (18,19).

Due to the arrangement of the muscle cells in the DGP model, the cells lacked coordination, which would have strongly affected their contraction and transmission functions; the severe damage to the structure of the muscle cells would also have been associated with a decline in function. At the same time, the energy supply of the muscle cells would have been affected due to lesions within the mitochondria. The reduction in cell function due to the above factors would have led to the inevitable result of a series of gastrointestinal motility disorder reactions, such as stomach dysrhythmia, increased gastric relaxation, easy expansion, weakness, propagation delay, wall thickening and luminal expansion (20,21). Delayed gastric emptying is a complication that can lead to the difficulty of blood control in diabetes (22).

Compared with the model group, the mucosal and submucosal vascular congestion of the EA group were alleviated. In addition, the mucosal gland cells were arranged in an orderly fashion with fewer vacuoles; the cell gaps were marginally larger, and there only existed a small amount of vacuolar degeneration on the gastric wall. The gastric SMCs of the EA-group rats were more orderly arranged than those of the model group; the large, soluble vacuoles within the cytoplasm of the muscle cells were rare and the mitochondrial swelling was not obvious. The electron densities in the gastric neurite and dendrite endings remained uniform. The myenteric plexus neurons were clear and the organelles, including the mitochondria and rough endoplasmic reticulum, remained abundant. It was also found that the number of gastric ICCs in the EA group was greater than that in the model group. It has been suggested that the acceleration of intestinal transition may increase the numbers of ICCs (23). The pathological damage to the ICCs, as well as the nerve endings between ICCs and SMCs, was less than that in the model group, and the structures were more distinct and tightly connected. The distribution of intramural nerves and ICCs, as well as the

pathological damage to the process connections, was reduced compared with that in the model group. The gastric capillary wall of the rats was uneven; the endothelial cell swelling and luminal congestion and bending were reduced; and there was less vacuolar degeneration.

The changes of gastric ICCs in the model group observed in the present study are consistent with the results of previous studies (24,25). EA can reduce the pathological damage to the gastric antrum in DGP rats, and has been shown to have a positive effect on the number and morphology of ICCs. A limitation of the present study, however, was that the findings did not clarify whether this effect is achieved through the acupuncture, local action of electric stimulation, or both; therefore, the precise mechanism of the effects of EA on ICCs, requires further investigation.

The experimental results of the present study showed that EA could adjust the ultrastructural changes of the gastric ICCs of the DGP model group, thus accelerating gastric emptying and improving the gastric motility disorders of the DGP rats. In conclusion, EA could reverse the cellular pathological damage to gastric tissue layers in the STZ diabetic rat model.

References

1. Forster J, Damjanov I, Lin Z, Sarosiek I, Wetzel P and McCallum RW: Absence of the interstitial cells of Cajal in patients with gastroparesis and correlation with clinical findings. J Gastrointest Surg 9: 102-108, 2005.
2. Grover M, Farrugia G, Lurken MS, Bernard CE, Faussone-Pellegrini MS, Smyrk TC, Parkman HP, Abell TL, Snape WJ, Hasler WL, *et al*; NIDDK Gastroparesis Clinical Research Consortium: Cellular changes in diabetic and idiopathic gastroparesis. Gastroenterology 140: 1575-1585, 2011.
3. Oh JH and Pasricha PJ: Recent advances in the pathophysiology and treatment of gastroparesis. J Neurogastroenterol Motil 19: 18-24, 2013.
4. Ordög T, Takayama I, Cheung WK, Ward SM and Sanders KM: Remodeling of networks of interstitial cells of Cajal in a murine model of diabetic gastroparesis. Diabetes 49: 1731-1739, 2000.
5. Gangula PR, Sekhar KR and Mukhopadhyay S: Gender bias in gastroparesis: Is nitric oxide the answer? Dig Dis Sci 56: 2520-2527, 2011.
6. Thazhath SS, Jones KL, Horowitz M and Rayner CK: Diabetic gastroparesis: Recent insights into pathophysiology and implications for management. Expert Rev Gastroenterol Hepatol 7: 127-139, 2013.
7. Iwasaki H, Kajimura M, Osawa S, Kanaoka S, Furuta T, Ikuma M and Hishida A: A deficiency of gastric interstitial cells of Cajal accompanied by decreased expression of neuronal nitric oxide synthase and substance P in patients with type 2 diabetes mellitus. J Gastroenterol 41: 1076-1087, 2006.
8. Wang C P, Kao C H, Chen W K, *et al*: A single-blinded, randomized pilot study evaluating effects of electroacupuncture in diabetic patients with symptoms suggestive of gastroparesis. J Altern Complement Med 14: 833-839, 2008.
9. Wang CP, Kao CH, Chen WK, Lo WY and Hsieh CL: A single-blinded, randomized pilot study evaluating effects of electroacupuncture in diabetic patients with symptoms suggestive of gastroparesis. J Altern Complement Med 14: 833-839, 2008.
10. Yang M, Li X, Liu S, Li Z, Xue M, Gao D, Li X and Yang S: Meta-analysis of acupuncture for relieving non-organic dyspeptic symptoms suggestive of diabetic gastroparesis. BMC Complement Altern Med 13: 311, 2013.
11. Lyford GL, He CL, Soffer E, Hull TL, Strong SA, Senagore AJ, Burgart LJ, Young-Fadok T, Szurszewski JH and Farrugia G: Pan-colonic decrease in interstitial cells of Cajal in patients with slow transit constipation. Gut 51: 496-501, 2002.
12. Sun JH, Guo H, Chen L, Wu XL, Li H, Pei LX, Peng YJ and Lu B: Effect of electroacupuncture at 'Tianshu' (ST 25) on colonic smooth muscle structure and interstitial cells of Cajal in slow transit constipation rats. Zhen Ci Yan Jiu 36: 171-175, 2011 (In Chinese).
13. Yang Q, Chen HQ, Huang YX, Wang W and Wang JJ: Effect of electroacupuncture-regulated gastric motility on interstitial cells of Cajal. Progr Mod Biomed 9: 1676-1678, 2009.
14. Jin QH, Shen HX, Wang H, Shou QY and Liu Q: Curcumin improves expression of SCF/c-kit through attenuating oxidative stress and NF-κB activation in gastric tissues of diabetic gastroparesis rats. Diabetol Metab Syndr 5: 12, 2013.
15. Lee J, Cummings BP, Martin E, Sharp JW, Graham JL, Stanhope KL, Havel PJ and Raybould HE: Glucose sensing by gut endocrine cells and activation of the vagal afferent pathway is impaired in a rodent model of type 2 diabetes mellitus. Am J Physiol Regul Integr Comp Physiol 302: 657-666, 2012.
16. Hua XB, Li CR, Zhou HL, *et al*: Experimental animal acupoint map. Shi Yan Dong Wu Yu Dong Wu Shi Yan 1: 1-5, 1991 (In Chinese).
17. He C, Soffer EE, Ferris CD, Walsh RM, Szurszewski JH and Farrugia G: Loss of interstitial cells of Cajal and inhibitory innervation in insulin-dependent diabetes. Gastroenterology 121: 427-434, 2001.
18. Horváth VJ, Vittal H and Ördög T: Reduced insulin and IGF-I signaling, not hyperglycemia, underlies the diabetes-associated depletion of interstitial cells of Cajal in the murine stomach. Diabetes 54: 1528-1533, 2005.
19. Horváth VJ, Vittal H, Lörincz A, Chen H, Almeida-Porada G, Redelman D and Ordög T: Reduced stem cell factor links smooth myopathy and loss of interstitial cells of cajal in murine diabetic gastroparesis. Gastroenterology 130: 759-770, 2006.
20. Ordög T: Interstitial cells of Cajal in diabetic gastroenteropathy. Neurogastroenterol Motil 20: 8-18, 2008.
21. Long QL, Fang DC, Shi HT and Luo YH: Gastro-electric dysrhythm and lack of gastric interstitial cells of Cajal. World J Gastroenterol 10: 1227-1230, 2004.
22. Choi KM, Gibbons SJ, Nguyen TV, Stoltz GJ, Lurken MS, Ordog T, Szurszewski JH and Farrugia G: Heme oxygenase-1 protects interstitial cells of Cajal from oxidative stress and reverses diabetic gastroparesis. Gastroenterology 135: 2055-2064, 2008.
23. Bellier S, Da Silva NR, Aubin-Houzelstein G, Elbaz C, Vanderwinden JM and Panthier JJ: Accelerated intestinal transit in inbred mice with an increased number of interstitial cells of Cajal. Am J Physiol Gastrointest Liver Physiol 288: 151-158, 2005.
24. Wu QX, Zhao M, Tan ZR, Qin LR, Huang X and Zhang HJ: Changes of interstitial cells of Cajal and connexin 43 expression in the gastric antrum of rats with diabetic gastroparesis: Implications for interventional effect of insulin. World J Gastroentero 22: 4399-4405, 2014.
25. Li N, Liu JM, Zhou HJ, *et al*: Effects of 'Shuang Gu Yi Tong' acupuncture on electrogastrogram and expression of gastric interstitial cells in rats with diabetic gastroparesis. Zhong Hua Zhong Yi Yao Xue Kan 32: 1855-1857, 2014 (In Chinese).